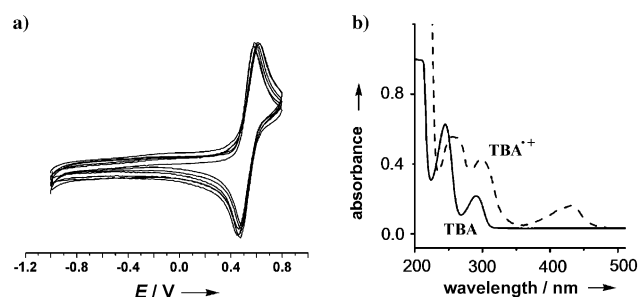


# Synthesis, Characterization, and Structures of a Persistent Aniline Radical Cation\*\*

Xiaoyu Chen, Xingyong Wang, Yunxia Sui, Yizhi Li, Jing Ma,\* Jinglin Zuo, and Xinpeng Wang\*

In contrast to *p*-phenyldiamine radical cations (Würster's salts),<sup>[1]</sup> aniline radical cations ( $\text{ArNR}_2^+$ ,  $\text{R} = \text{H}$  or alkyl) are highly reactive and often exist as short-lived intermediates occurring in dimerization,<sup>[2]</sup> cationic polymerization,<sup>[3]</sup> azo compound formation,<sup>[4]</sup> benzidine rearrangement,<sup>[5]</sup> proton-transfer reactions,<sup>[6,7]</sup> and various nucleophilic substitutions such as nitration,<sup>[7]</sup> methoxylation,<sup>[8]</sup> cyanation,<sup>[9]</sup> and halogenation.<sup>[2b]</sup> Because of their importance, aniline radical cations have been the subject of numerous theoretical<sup>[10]</sup> and experimental studies in the gas phase<sup>[10]</sup> and in solution.<sup>[6–9,11]</sup> Calculations have predicted that a discrete aniline radical cation in the gas phase adopts a planar quinoidal-type structure with a partial double C–N bond and the unpaired electron is delocalized in the phenyl ring.<sup>[10]</sup> However, isolation of salts with an aniline radical cation remains a challenge. By using weakly coordinating anions,<sup>[12]</sup> we have previously succeeded in isolating benzidine radical cations.<sup>[13]</sup> We herein report the synthesis, characterization, and structures of an aniline radical cation  $\text{TBA}^+$  ( $\text{TBA} = 2,4,6\text{-}t\text{-Bu}_3\text{C}_6\text{H}_2\text{NH}_2$ ), stabilized both in the solution and solid states. The cation exists as two isomers that interchange at different temperatures and features an exceptionally long C–N bond longer than that predicted by theory.

Cyclic voltammetry of TBA in  $\text{CH}_2\text{Cl}_2$  at room temperature with 0.1 M  $\text{Bu}_4\text{NPF}_6$  as the supporting electrolyte showed well-defined reversible oxidation waves (Figure 1 a), indicating that the radical cation  $\text{TBA}^+$  is stable under these conditions.<sup>[14]</sup> Upon one-electron oxidation with  $\text{AgSbF}_6$  in  $\text{CH}_2\text{Cl}_2$ , TBA was converted to a green radical cation salt  $\text{TBA}^+\text{SbF}_6^-$  in considerable yield [Eq. (1)]. In contrast,



**Figure 1.** a) Cyclic voltammograms of TBA in  $\text{CH}_2\text{Cl}_2$  ( $2 \times 10^{-4}$  M, 0.1 M  $\text{Bu}_4\text{NPF}_6$ , 298 K) were measured at various scan rates: 50, 100, 200, 300, 400, 500  $\text{mV s}^{-1}$ . For a colored drawing, see Figure S1 in the Supporting Information. b) Absorption spectra of TBA ( $1 \times 10^{-4}$  M) and  $\text{TBA}^+\text{SbF}_6^-$  ( $1 \times 10^{-4}$  M) in  $\text{CH}_2\text{Cl}_2$  at 298 K.



TBA = 2, 4, 6-*t*- $\text{Bu}_3\text{C}_6\text{H}_2\text{NH}_2$

attempts to stabilize the aniline radical cation with other anions such as  $\text{BF}_4^-$  and  $\text{CF}_3\text{SO}_3^-$  failed.<sup>[15]</sup> On the basis of the literature<sup>[2b,16]</sup> and in comparison to the electronic absorption of the neutral TBA, the band at  $432 \text{ cm}^{-1}$  in the absorption spectrum (expt. Figure 1 b; calc. Figure S15b in the Supporting Information) was assigned to the radical cation  $\text{TBA}^+$ . The simulated EPR spectrum is in good agreement with the experimental EPR spectrum, revealing a pattern resulting from interactions of the electron with H (of  $\text{NH}_2$  and the phenyl ring) and N atoms (Figure 2).<sup>[17]</sup> The solid-state EPR spectrum shows one single line with  $g = 2.0039$  (Figure S3 in the Supporting Information).

Green crystals suitable for X-ray crystallographic studies were obtained from dichloromethane solutions of  $\text{TBA}^+\text{SbF}_6^-$  at  $-20^\circ\text{C}$ . Single-crystal structures of  $\text{TBA}^+\text{SbF}_6^-$  were determined at various temperatures: 123, 223, 273, 296, 323, 353, and 373 K.<sup>[18]</sup> The crystal maintained the orthorhombic space group  $Pmn2_1$ . The monomeric radical cation  $\text{TBA}^+$  is regularly stacked along the *b* axis by C–H $\cdots\pi$  intermolecular interactions. The interplanar distances are around 5.1 Å, much larger than the equilibrium van der Waals separation of 3.4 Å, indicating that there are no intermolecular  $\pi$ – $\pi$  interactions (Figure S6 in the Supporting Information). The phenyl ring of the  $\text{TBA}^+$  radical cation (Figure 3 and Table 1) is distorted with respect to that of neutral TBA,<sup>[19]</sup> but upon heating it maintains  $C_s$  symmetry with the mirror plane bisecting the phenyl ring. At 123 K the

[\*] X. Chen, Dr. Y. Sui, Prof. Y. Li, Prof. J. Zuo, Prof. X. Wang  
State Key Laboratory of Coordination Chemistry  
Nanjing National Laboratory of Microstructures  
Nanjing University, Nanjing 210093 (China)  
E-mail: xpwang@nju.edu.cn

Dr. X. Wang, Prof. J. Ma  
Theoretical and Computational Chemistry Institute  
School of Chemistry and Chemical Engineering  
Nanjing University, Nanjing 210093 (China)  
E-mail: majing@nju.edu.cn

[\*\*] We thank the National Natural Science Foundation of China (grants 21171087 and 91122019 to X.W.; 20725104 to J.Z., and 20825312 to J.M.), the Natural Science Foundation of Jiangsu Province (grant BK2011549 to X.W.), 1000 Young Talent Program (grant to X.W.), and the National Basic Research Program (grant 2011CB808604 to J.M.) for financial support. We are grateful to the High Performance Computing Centre of Nanjing University for providing the IBM Blade cluster system. Part of the computational work has been done on the Sugon TC5000 high performance linux cluster at ITCC.

Supporting information for this article is available on the WWW under <http://dx.doi.org/10.1002/anie.201205478>.

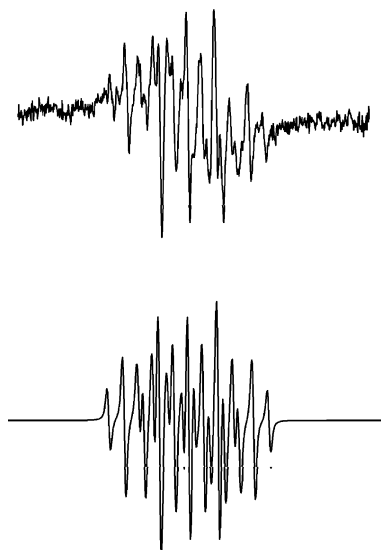


**Figure 2.** Experimental (top;  $\text{CH}_2\text{Cl}_2$ ,  $1 \times 10^{-4}$  M, 233 K) and simulated (bottom) EPR spectra of  $\text{TBA}^{\bullet+}$  with  $a_{\text{N}} = 5.48$  G,  $a_{\text{H}}^{\text{NH}} = 6.62$  G (2 H),  $a_{\text{H}}^{\text{C}_6\text{H}_2} = 2.90$  G (2 H).

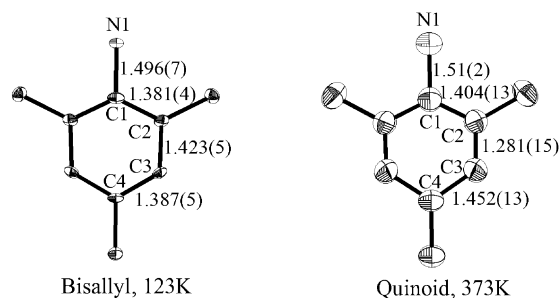
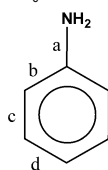


**Figure 3.** The X-ray structures (bond lengths in Å) of the  $\text{TBA}^{\bullet+}$  cation in  $\text{TBA}^{\bullet+}\text{SbF}_6^-$  at different temperatures. Ellipsoids are drawn at the 30% probability level. Hydrogen atoms and some carbon atoms of the *t*Bu groups are not shown.

**Table 1:** Experimental bond lengths [Å] of neutral aniline TBA and its radical cation  $\text{TBA}^{\bullet+}$  in  $\text{TBA}^{\bullet+}\text{SbF}_6^-$ .

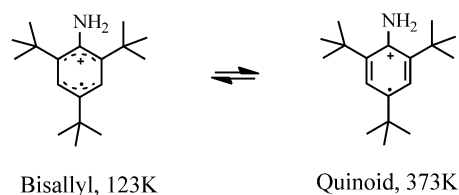


Bond	TBA (150 K) [a]	$\text{TBA}^{\bullet+}$ (123 K)	$\text{TBA}^{\bullet+}$ (373 K)
a(C1–N1)	1.415(3)	1.496(7)	1.51(2)
b(C1–C2)	1.414(2)	1.381(4)	1.404(13)
c(C2–C3)	1.395(2)	1.423(5)	1.281(15)
d(C3–C4)	1.386(2)	1.387(5)	1.452(13)

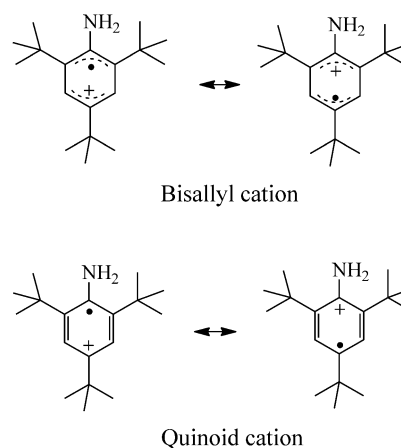
[a] Ref. [19].

longitudinal bond (labeled c in Table 1) inside the ring is elongated while one of the transverse bonds (b) is contracted, leading to a bisallyl-type structure. The bond-length variations within the phenyl ring are above the error limits. When the crystal is heated up, the transverse (b, d) and longitudinal

(c) bonds are elongated and shortened, respectively, resulting in the quinoid-type isomer at high temperatures (see Figure 3 for the structure at 373 K).<sup>[20]</sup> Although standard deviations at higher temperatures are large and this precluded the precise determination of the structural parameters, the trend of geometry change with increasing temperature is apparent (Figure S9). The process is completely reversed by cooling the crystal back to low temperatures (Scheme 1). The geometries of the bisallyl and quinoid isomers can be represented by the Lewis structures shown in Scheme 2. It is worthwhile to note that the C–N bond (a, ca. 1.5 Å) basically remains the same length throughout the temperature range, and is considerably longer than that (1.415(3) Å) of the neutral aniline.<sup>[19]</sup>



**Scheme 1.** Temperature-dependent structural transitions of the radical cation  $\text{TBA}^{\bullet+}$ .



**Scheme 2.** The Lewis structures for the bisallyl and quinoid isomers.

To rule out the possibility that the crystal might contain the N-protonated 1,3,5-tri-*tert*-butylanilinium cation ( $\text{TBAH}^+$ ), we prepared  $\text{TBAH}^+\text{SbF}_6^-$  on purpose by the reaction of  $(\text{TBAH})\text{Cl}$  with  $\text{AgSbF}_6$  (1:1). Colorless crystals (Figure S4 in the Supporting Information) of  $\text{TBAH}^+\text{SbF}_6^-$  suitable for X-ray crystallographic studies were obtained from dichloromethane solutions and several crystals were investigated.<sup>[21]</sup> The unit cell parameters and space group, together with the lack of color and EPR silence of  $\text{TBAH}^+\text{SbF}_6^-$  are different from those of the crystals of  $\text{TBA}^{\bullet+}\text{SbF}_6^-$ . In addition, the X-ray structure analysis of  $\text{TBAH}^+\text{SbF}_6^-$  at higher temperatures (296 and 373 K) was also conducted and all bond lengths were found to be slightly elongated due to thermal expansion (Figure S10). This is in sharp contrast to the change in bond length alternations within phenyl rings of

TBA<sup>+</sup>SbF<sub>6</sub><sup>−</sup> upon heating. Thus any possibility for N-protonated 1,3,5-tri-*tert*-butylanilinium cation (TBAH<sup>+</sup>) has been completely excluded.

To rationalize the experimental results, we carried out some calculations on the isolated species and cation–anion complexes.<sup>[22]</sup> Full geometry optimizations were obtained and the obtained stationary points were characterized by frequency calculations. Similar to the calculated parent aniline radical cation C<sub>6</sub>H<sub>5</sub>NH<sub>2</sub><sup>•+</sup>,<sup>[10]</sup> the isolated radical cation TBA<sup>•+</sup>, optimized at UB3LYP, UM06-2X, and UMP2/6-31G(d) levels, has a planar quinoidal-type structure with a partial C–N double bond (Figure 4a; Figures S11 and 12 in

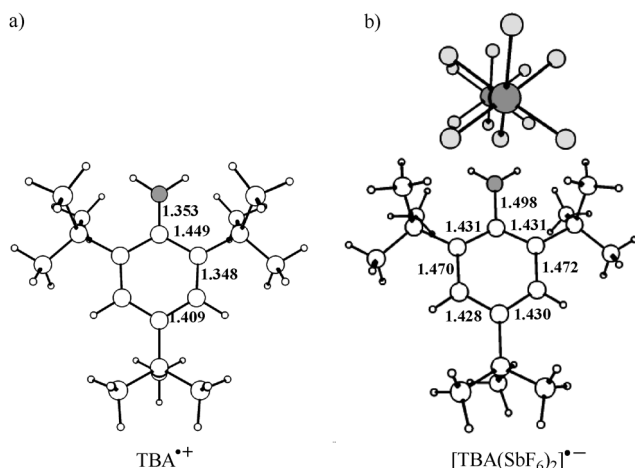


**Figure 4.** Calculated geometries (bond lengths in Å) of a) discrete TBA<sup>•+</sup> radical cation and b) [TBA(SbF<sub>6</sub>)<sub>2</sub>]<sup>•−</sup> complex at the level of UMP2/6-31G(d) (LANL2DZ for Sb).

the Supporting Information). This C–N bond (1.353 Å) is considerably shorter than that (1.5 Å) in the solid state. The experimental geometry of TBA<sup>•+</sup> can be reproduced only when two SbF<sub>6</sub><sup>−</sup> anions are included into calculation (Figure 4b) at the UMP2/6-31G(d) level (LANL2DZ for Sb), which strongly indicates that the stabilization of the radical cation TBA<sup>•+</sup> and its structural deviation from the gas-phase geometry may arise from a special crystal environment or the crystal packing forces. In addition, the anion interacts strongly enough to distort the structure of the cation beyond the theoretical prediction on a discrete cation. The elongation of the C–N bond is probably caused by the electrostatic interaction, which weakens the N<sub>lone pair</sub> → π<sub>phen</sub><sup>\*</sup> negative hyperconjugation. Natural bond orbital (NBO) analysis supports this point (see the Supporting Information). However, it is difficult to study the influence of the anions on the cations at different temperatures as the SbF<sub>6</sub><sup>−</sup> anions are disordered upon heating (Figure S8). Nonetheless the Lewis structures of quinoidal and bisallyl isomers are supported by the calculated two highest occupied orbitals (Figure 5) using experimental geometries taken from X-ray structures.

The control of molecular properties by governing valence electrons is important for chemical reactions and building molecular devices.<sup>[23]</sup> This can be studied by quantum calculations. For example, aromaticity of benzene can be

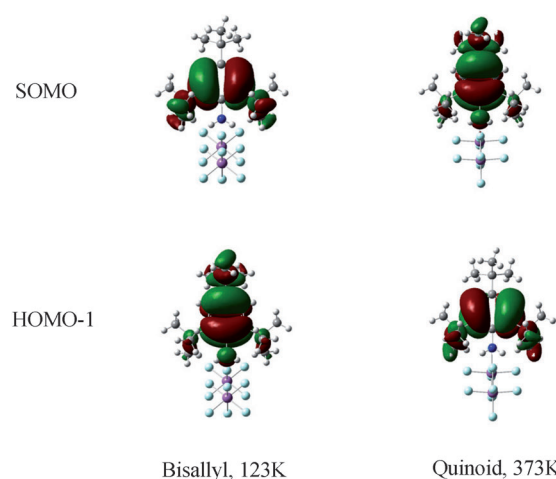


**Figure 5.** View of the two highest occupied orbitals of the bisallyl and quinoid isomers with two SbF<sub>6</sub><sup>−</sup> anions, calculated at the level of UMP2/6-31G(d) (LANL2DZ for Sb). For the quinoid structure, fluorine atoms with higher occupancy were used.

controlled by electron dynamics.<sup>[24]</sup> Theoretical studies have shown that the loss of one electron from benzene or its derivatives could lead to either a quinoid or a bisallyl structure owing to the Jahn–Teller effect.<sup>[25]</sup> Quite recently, Seppelt et al. reported the C<sub>6</sub>F<sub>6</sub><sup>•+</sup> radical cation in both the quinoid and the bisallyl isomeric forms coexisting in one crystal.<sup>[26]</sup> Whether these two isomers interchange has not yet been tested experimentally.

In conclusion, the green color (solid and solution), EPR spectra, and electronic absorption imply that the aniline salt isolated is the radical cation salt TBA<sup>•+</sup>SbF<sub>6</sub><sup>−</sup>, which has also been successfully isolated as stable crystals and studied by X-ray crystallography. This compound undergoes reversible isomerization upon heating or cooling in the solid state, which is unprecedented for a simple phenyl ring system and implies that the valence electrons of the radical cation can be controlled by temperature. We have described the first example of an aniline radical cation in the solid state, which may be used as a stable intermediate for model studies.<sup>[2–9]</sup>

## Experimental Section

### General Procedures

All experiments were carried out under a nitrogen atmosphere using standard Schlenk techniques and a glove box. 2,4,6-*t*Bu<sub>3</sub>C<sub>6</sub>H<sub>2</sub>NH<sub>2</sub> (TBA, Alfa Aesar) and AgSbF<sub>6</sub> (Alfa Aesar) were purchased and used without further purification. Solvents were dried prior to use. Cyclic voltammetry was performed on an IM6ex electrochemical workstation, with platinum as the working and counter electrodes, Ag/Ag<sup>+</sup> as the reference electrode, and 0.1M *n*Bu<sub>4</sub>NPF<sub>6</sub> as the supporting electrolyte. EPR spectra were obtained using a Bruker EMX-10/12 variable-temperature apparatus. UV/Vis spectra were recorded on a UV-3600 spectrophotometer. Elemental analyses were performed at Shanghai Institute of Organic Chemistry, the Chinese Academy of Sciences. X-ray crystal structures were obtained with Bruker APEX DUO CCD detectors at different temperatures. Single crystals were coated with Paratone-N oil and mounted using a glass

fiber and AB glue. TGA was performed using a Netzsch Sta 449c thermal analyzer system at a heating rate of  $10^{\circ}\text{Cmin}^{-1}$  in  $\text{N}_2$  atmosphere.

$\text{TBA}^+\text{SbF}_6^-$ : Under anaerobic and anhydrous conditions, a mixture of TBA (0.102 g, 0.390 mmol) and  $\text{AgSbF}_6$  (0.129 g, 0.375 mmol) in  $\text{CH}_2\text{Cl}_2$  (ca. 60 mL) was stirred at room temperature for 1 day. A gray precipitate (Ag metal) was filtered off of the resultant green solution. The filtrate was then concentrated and stored at roughly  $-20^{\circ}\text{C}$  for 1 day to afford X-ray-quality crystals of the radical cation salt  $\text{TBA}^+\text{SbF}_6^-$ . Yield: 0.159 g, 82%; m.p.  $172\text{--}174^{\circ}\text{C}$ ; elemental analysis (%): calcd C 43.47, H 6.24, N 2.82; found C 43.42, H 6.46, N 2.89.

Received: July 11, 2012

Published online: October 19, 2012

**Keywords:** anilines · isomers · radical ions · structure elucidation

- [1] a) C. Wurster, R. Sendtner, *Ber. Dtsch. Chem. Ges.* **1879**, 12, 1803; b) L. Michaelis, M. P. Schubert, S. Granick, *J. Am. Chem. Soc.* **1939**, 61, 1981–1992.
- [2] a) R. L. Hand, R. F. Nelson, *J. Am. Chem. Soc.* **1974**, 96, 850–860; b) M. Kirchgessner, K. Sreenath, K. R. Gopidas, *J. Org. Chem.* **2006**, 71, 9849–9852.
- [3] R. R. Bodalia, R. S. Duran, *J. Am. Chem. Soc.* **1993**, 115, 11467–11474.
- [4] A. Grirrane, A. Corma, H. Garcia, *Science* **2008**, 322, 1661–1664.
- [5] H. J. Shine, H. Zmuda, K. H. Park, H. Kwart, A. G. Horgan, M. Brechbiel, *J. Am. Chem. Soc.* **1982**, 104, 2501–2509.
- [6] V. D. Parker, M. Tilset, *J. Am. Chem. Soc.* **1991**, 113, 8778–8781.
- [7] R. N. Loepky, S. P. Singh, S. Elomari, R. Hastings, T. E. Theiss, *J. Am. Chem. Soc.* **1998**, 120, 5193–5202.
- [8] J. Tsuji, K. Ohno, *J. Am. Chem. Soc.* **1968**, 90, 91–94.
- [9] S. Andreades, E. W. Zahnow, *J. Am. Chem. Soc.* **1969**, 91, 4181–4190.
- [10] a) G. N. R. Tripathi, R. H. Schuler, *J. Chem. Phys.* **1987**, 86, 3795–3800; b) A. M. Brouwer, R. Wilbrandt, *J. Phys. Chem.* **1996**, 100, 9678–9688; c) P. Karafiloglou, J. Launay, *J. Phys. Chem. A* **1998**, 102, 8004–8012; d) P. M. Wojciechowski, W. Zierkiewicz, D. Michalska, P. Hobza, *J. Chem. Phys.* **2003**, 118, 10900–10911; e) A. Maroz, R. Hermann, S. Naumov, O. Brede, *J. Phys. Chem. A* **2005**, 109, 4690–4696.
- [11] a) D. M. Mohilner, R. N. Adams, W. J. Argersinger, *J. Am. Chem. Soc.* **1962**, 84, 3618–3622; b) T. Mizoguchi, R. N. Adams, *J. Am. Chem. Soc.* **1962**, 84, 4181–4190; c) J. Bacon, R. N. Adams, *J. Am. Chem. Soc.* **1968**, 90, 6596–6599; d) M. J. Drews, P. S. Wong, P. R. Jones, *J. Am. Chem. Soc.* **1972**, 94, 9122–9128; e) M. Jonsson, J. Lind, T. E. Eriksen, G. Merényi, *J. Am. Chem. Soc.* **1994**, 116, 1423–1427; f) A. Yu, Y. Liu, Z. Li, J. Cheng, *J. Phys. Chem. A* **2007**, 111, 9978–9987.
- [12] a) I. Krossing, I. Raabe, *Angew. Chem.* **2004**, 116, 2116–2142; *Angew. Chem. Int. Ed.* **2004**, 43, 2066–2090; b) T. S. Cameron, J. Passmore, X. Wang, *Angew. Chem.* **2004**, 116, 2029–2032; *Angew. Chem. Int. Ed.* **2004**, 43, 1995–1998; c) A. Decken, J. Passmore, X. Wang, *Angew. Chem.* **2006**, 118, 2839–2843; *Angew. Chem. Int. Ed.* **2006**, 45, 2773–2777; d) X. Wang, P. Peng, M. Olmstead, H. Hope, P. P. Power, *J. Am. Chem. Soc.* **2010**, 132, 13150–13151.
- [13] X. Chen, B. Ma, X. Wang, S. Yao, L. Ni, Z. Zhou, Y. Li, W. Huang, J. Ma, J. Zuo, X. Wang, *Chem. Eur. J.* **2012**, 18, 11828–11836.
- [14] Cyclic voltammetry of TBA at a higher concentration in  $\text{CH}_2\text{Cl}_2$  shows slight shifts of oxidation potentials in various scans (50–500  $\text{mVs}^{-1}$ ) but no reversible dimerization of the aniline radical cation was found (Figure S1 in the Supporting Information), which is probably a result of steric hindrance. For an example of the reversible dimerization of an amine radical cation, see: O. Yurchenko, J. Heinze, S. Ludwigs, *ChemPhysChem* **2010**, 11, 1637–1640.
- [15] The green reaction solution of TBA with the large weakly coordinating anion salt  $\text{Ag}[\text{Al}(\text{OC}(\text{CF}_3)_3)_4]$  did not crystallize, while that of TBA with  $\text{AgSO}_3\text{CF}_3$  or  $\text{AgBF}_4$  rapidly turned colorless in a few minutes.
- [16] T. Shida, *Electronic Absorption Spectra of Radical Ions*, Elsevier, Amsterdam, **1988**, p. 209.
- [17] F. Neugebauer, S. Bamberger, W. Groh, *Tetrahedron Lett.* **1973**, 14, 2247–2248.
- [18] X-ray data for  $\text{TBA}^+\text{SbF}_6^-$  at 123 K ( $\text{C}_{18}\text{H}_{31}\text{NSbF}_6$ , FW = 497.2,  $\text{Mo}_{\text{K}\alpha}$ ,  $\lambda = 0.71073 \text{ \AA}$ ), orthorhombic, space group  $\text{Pmn}2_1$ ,  $Z = 2$ ,  $\mu = 1.314 \text{ mm}^{-1}$ ,  $a = 13.8670(12)$ ,  $b = 5.9971(11)$ ,  $c = 13.1290(16) \text{ \AA}$ ,  $V = 1091.8(3) \text{ \AA}^3$ ,  $R1 = 0.0273$  for 1406 ( $I > 2\sigma(I)$ ) reflections,  $wR2 = 0.0571$  (all data);  $T = 373 \text{ K}$ , orthorhombic, space group  $\text{Pmn}2_1$ ,  $Z = 2$ ,  $\mu = 1.272 \text{ mm}^{-1}$ ,  $a = 13.710(4)$ ,  $b = 6.176(2)$ ,  $c = 13.329(4) \text{ \AA}$ ,  $V = 1128.5(6) \text{ \AA}^3$ ,  $R1 = 0.0739$  for 1079 ( $I > 2\sigma(I)$ ) reflections,  $wR2 = 0.1788$  (all data). For data at other temperatures, see Table S1 in the Supporting Information.
- [19] E. Pohl, R. Herbstirmer, K. Kohler, H. W. Roesky, G. M. Sheldrick, *Acta Crystallogr. Sect. C* **1993**, 49, 2141–2143.
- [20] a) The single-crystal structures of  $\text{TBA}^+\text{SbF}_6^-$  determined at other temperatures between 123–373 K were found to be close to either the bisallyl or quinoid structure or in between. It seems that 296 K is the transition temperature at which the isomerism between bisallyl and quinoid structures occurs (Figure S9 in the Supporting Information); b) To test the thermal stability of crystals of  $\text{TBA}^+\text{SbF}_6^-$ , TGA of crystals was performed and showed no weight loss on the X-ray time scale (Figure S5); c) A libration analysis was performed on the structure at 373 K to give corrections of 0.002  $\text{\AA}$  for the bonds C2–C3 and C1–N1, –0.001  $\text{\AA}$  for the bond C1–C2, and 0.001  $\text{\AA}$  for the bond C3–C4.
- [21] The X-ray data of  $\text{TBA}^+\text{SbF}_6^-$  is compared with that of  $\text{TBAH}^+\text{SbF}_6^-$  in Tables S1 and S2 in the Supporting Information. X-ray data for  $\text{TBAH}^+\text{SbF}_6^-$  ( $\text{C}_{18}\text{H}_{32}\text{NSbF}_6$ , FW = 498.2,  $\text{Mo}_{\text{K}\alpha}$ ,  $\lambda = 0.71073 \text{ \AA}$ ) at 123 K: monoclinic, space group  $\text{P}2_1/\text{m}$ ,  $Z = 2$ ,  $\mu = 1.293 \text{ mm}^{-1}$ ,  $a = 5.954(5)$ ,  $b = 14.315(11)$ ,  $c = 13.040(10) \text{ \AA}$ ,  $\beta = 92.804(13)$ ,  $V = 1110.1(15) \text{ \AA}^3$ ,  $R1 = 0.0494$  for 1940 ( $I > 2\sigma(I)$ ) reflections,  $wR2 = 0.1201$  (all data). For X-ray data of  $\text{TBAH}^+\text{SbF}_6^-$  at other temperatures see Table S2. The preparation and full characterization of  $\text{TBAH}^+\text{SbF}_6^-$  will be published elsewhere. CCDC 865462, 865463, 865464, 890319, 890320, 890321, 890322 ( $\text{TBA}^+\text{SbF}_6^-$ ), 873366, 890317, 890318 ( $\text{TBAH}^+\text{SbF}_6^-$ ) contain the supplementary crystallographic data for this paper. These data can be obtained free of charge from The Cambridge Crystallographic Data Centre via [www.ccdc.cam.ac.uk/data\\_request/cif](http://www.ccdc.cam.ac.uk/data_request/cif).
- [22] All calculations were performed using the Gaussian 09 program suite. M. J. Frisch, et al. Gaussian09, Revision B.01; Gaussian, Inc.: Wallingford, CT **2010**. See the Supporting Information for details.
- [23] B. L. Feringa, *Molecular Switches*, Wiley-VCH, Weinheim, **2001**.
- [24] I. S. Ulusoy, M. Nest, *J. Am. Chem. Soc.* **2011**, 133, 20230–20236, and references therein.
- [25] I. B. Bersuker, *Chem. Rev.* **2001**, 101, 1067–1114, and references therein.
- [26] H. Shorafa, D. Mollenhauer, B. Paulus, K. Seppelt, *Angew. Chem.* **2009**, 121, 5959–5961; *Angew. Chem. Int. Ed.* **2009**, 48, 5845–5847.